Impact of optimized PET imaging conditions on F-18-FDG uptake quantification in patients with apparently normal aortas

Lawal, Ismaheel O.; Mokoala, Kgomotso G.; Popoola, Gbenga O.; Lengana, Thabo; Ankrah, Alfred O.; Stoltz, Anton C.; Sathekge, Mike M.

Published in:
Journal of Nuclear Cardiology

DOI:
10.1007/s12350-019-01833-6

Impact of optimized PET imaging conditions on ^{18}F-FDG uptake quantification in patients with apparently normal aortas

Ismaheel O. Lawal, MD,[a] Kgomotso G. Mokoala, MD,[a] Gbenga O. Popoola, MD,[b] Thabo Lengana, MD,[a] Alfred O. Ankrah, MD,[a,c] Anton C. Stoltz, MD, PhD,[d] and Mike M. Sathekge, MD, PhD[a]

[a] Department of Nuclear Medicine, University of Pretoria and Steve Biko Academic Hospital, Pretoria, South Africa
[b] Department of Epidemiology and Community Health, University of Ilorin, Ilorin, Nigeria
[c] Department of Nuclear Medicine and Molecular Imaging, University Medical Center Groningen, University of Groningen, Groningen, The Netherlands
[d] Infectious Disease Unit, Department of Internal Medicine, University of Pretoria and Steve Biko Academic Hospital, Pretoria, South Africa

Received Apr 28, 2019; accepted Jul 18, 2019
doi:10.1007/s12350-019-01833-6

Background. **The cardiovascular committee of the European Association of Nuclear Medicine (EANM) recently published recommendations on imaging conditions to be observed during ^{18}F-FDG PET imaging of vascular inflammation. This study aimed to evaluate the impact of applying these optimized imaging conditions on PET quantification of arterial ^{18}F-FDG uptake.**

Methods and Results. **Fifty-seven patients were prospectively recruited to undergo an early ^{18}F-FDG PET/CT imaging at 60 minutes and repeat delayed imaging at ≥ 120 minutes post tracer injection. Routine oncologic ^{18}F-FDG PET protocol was observed for early imaging, while delayed imaging parameters were optimized for vascular inflammation imaging as recommended by the EANM. Aortic SUVmax of the ascending aorta and SUVmean from the lumen of the superior vena cava (SVC SUVmean) were obtained on early and delayed imaging. Target-to-background ratio (TBR) was obtained for the early and delayed imaging. Aortic SUVmax increased by a mean of 70%, while SVC SUVmean decreased by a mean of 52% between early and delayed imaging ($P < 0.001$). TBR increased by 122% following delayed imaging. TBR increased, while SVC SUVmean declined across all time-points from 120 to > 180 minutes. Aortic SUVmax significantly increased at imaging time-points between 120 and 180 minutes. No significant improvement in aortic SUVmax was seen at imaging time-points beyond 180 minutes.**

Conclusions. **^{18}F-FDG PET imaging conditions optimized for vascular inflammation imaging lead to an improved quantification through an increase in the quantified vascular tracer uptake and decrease in blood-pool background activity. (J Nucl Cardiol 2021;28:1349–59.)**

Key Words: FDG • PET/CT • vascular inflammation • atherosclerosis • TBR

Electronic supplementary material The online version of this article (https://doi.org/10.1007/s12350-019-01833-6) contains supplementary material, which is available to authorized users.

The authors of this article have provided a PowerPoint file, available for download at SpringerLink, which summarizes the contents of the paper and is free for re-use at meetings and presentations. Search for the article DOI on SpringerLink.com.

The authors have also provided an audio summary of the article, which is available to download as ESM, or to listen to via the JNC/ASNC Podcast.

Reprint requests: Mike M. Sathekge, MD, PhD, Department of Nuclear Medicine, University of Pretoria and Steve Biko Academic Hospital, Private Bag X169, Pretoria 0001, South Africa; *mike.sathekge@up.ac.za*

J Nucl Cardiol
1071-3581/$34.00

Abbreviations	
CT	Computed tomography
EANM	European Association of Nuclear Medicine
^{18}F-FDG	Fluorine-18 fluorodeoxyglucose
MBq	Mega Becquerel
PET	Positron emission tomography
ROI	Region of interest
SVC	Superior vena cava
SUVmax	Maximum standardized uptake value
SUVmean	Mean standardized uptake value
TBR	Target-to-background ratio

See related editorial, pp. 1360–1363

INTRODUCTION

Atherosclerotic cardiovascular disease remains a significant cause of death globally.[1] Inflammation plays an essential role in the formation, progression, and complication of vascular atheromatous lesions.[2] Radionuclide methods are a viable tool for imaging of vascular inflammation.[3] Fluorine-18 Fluorodeoxyglucose (^{18}F-FDG) positron emission tomography with computed tomography (PET/CT) is the most used radionuclide technique for vascular and cardiac inflammation and infection imaging.[4] ^{18}F-FDG accumulates more in vessels of individuals at higher risk of cardiovascular disease.[5] In patients with established vascular atheroma, a higher level of ^{18}F-FDG uptake has been reported in symptomatic as compared with asymptomatic plaque. In asymptomatic plaque, the level of ^{18}F-FDG accumulation in the vascular lesions predicts future risk of vascular event.[6,7]

Despite the widespread use of ^{18}F-FDG PET/CT for vascular inflammation imaging for research purposes, many limitations militating against the accurate quantification of arterial ^{18}F-FDG uptake remain. The mean thickness of the arterial wall is often less than twice the spatial resolution of most clinical PET cameras, subjecting ^{18}F-FDG quantification to significant partial volume averaging.[8,9] Target-to-background ratio (TBR), a ratio of arterial ^{18}F-FDG uptake to blood-pool background activity, is the most commonly used parameter for quantifying arterial ^{18}F-FDG uptake. Delayed imaging beyond the typical 60-minute uptake time observed in oncologic PET imaging is often required to achieve an optimum arterial ^{18}F-FDG uptake and blood-pool background clearance.[10,11] Wide variability exists regarding the uptake time and other imaging parameters observed in reported studies.[8] Many studies have reported TBR obtained from routine PET imaging done for other indications.[5,7,12] Given this wide variability, the cardiovascular committee of the European Association of Nuclear Medicine (EANM) made a set of technical recommendations on imaging conditions that should be observed in PET imaging of atherosclerotic vascular inflammation.[13] One of the key elements of these recommendations is an uptake time of 120 minutes, significantly longer than the 60-minute uptake time for routine oncologic ^{18}F-FDG PET imaging. To date and to our knowledge, no study has been done to show that these recommended parameters, when observed, produce a better quantification of arterial ^{18}F-FDG. The aim of our study was, therefore, to evaluate the impact of optimized PET conditions on vascular uptake of ^{18}F-FDG quantification in vascular inflammation imaging.

METHODS

Patients

Patients referred to the Department of Nuclear Medicine at Steve Biko Academic Hospital for various indications between August and December 2018 were prospectively recruited to undergo two sets of ^{18}F-FDG PET/CT imaging. We recruited adults who had no pathology on their ^{18}F-FDG PET/CT imaging and whose blood sugar level was $\leq$ 7mmol/L at the time of intravenous injection of ^{18}F-FDG. Our exclusion criteria included use of anti-inflammatory therapy, active inflammation, or malignancy and renal failure (glomerular filtration rate $<$ 60mL/min/m^2). All patients signed informed consent to participate in the study. The research ethics committee of the faculty of health sciences, University of Pretoria approved the study.

Early PET/CT Imaging

Early imaging was done as per our routine departmental ^{18}F-FDG PET/CT imaging protocol for oncologic and inflammation/infection imaging. Briefly, all patients observed a minimum of 6 hours of fasting. Fasting blood sugar was obtained in all patients using a portable glucometer. The activity of ^{18}F-FDG administered was calculated using the formula: [(body weight in kg $\div$10) + 1] $\times$ 37 MBq corresponding to 3-4 MBq recommended in the EANM position paper.[13] After an uptake period of 60 minutes (median = 64, range = 60 to 69), a vertex to mid-thigh non-contrasted CT followed by PET imaging was performed using a hybrid Biograph Truepoint PET/CT camera (Siemens Medical Solution, IL, USA). CT parameters were as follows: tube voltage = 120 KeV, tube current = 40 mAs, sectional width = 5 mm and pitch = 0.8, matrix = 512 $\times$ 512. CT data were used for attenuation correction and anatomic co-localization. PET imaging was done in 3D mode at 3 minutes per bed position. PET images were reconstructed using ordered subset expectation maximization (OSEM) iterative reconstruction algorithm (8 iterations) with a Gaussian filter applied at 5.0 mm full width at half maximum.

Delayed PET/CT Imaging

Patients who had no evident pathology either due to infection or malignancy and who consented to participate in the study underwent delayed PET/CT imaging at ≥ 120 minutes post ^{18}F-FDG injection. CT imaging with similar parameters to those of the early PET/CT imaging was repeated for the delayed imaging. For the delayed PET imaging, two-bed positions over the chest were acquired at 8 minutes per bed position. No post-filtering was applied, and image reconstruction was performed with OSEM (120 iterations).

Image Analysis

All images were analyzed by a single experienced observer (IOL) on a dedicated Syngo.via workstation (Siemens medical solutions, IL, USA).[5] We used the ascending aorta as the artery of interest to quantify TBR. The fused PET/CT imaging images were used for image analysis to facilitate clear delineation of the vessels of interest and prevent count spill-over from adjacent structures. We drew multiple regions of interest (ROIs) encircling the ascending aorta from above the coronary ostia to its termination as it continues as the arch of the aorta. We obtained the mean of these measurements for the early and delayed imaging as aortic SUVmax_early and aortic SUVmax_late. We used the superior vena cava (SVC) as the vein of interest to compute the blood-pool background activity. We obtained SVC SUVmean from multiple ROIs drew within the lumen of the SVC at levels corresponding to the levels where SUVmax of ascending aorta was taken. We obtained the mean of these measurements on the early and delayed imaging as SVC SUVmean_early and SVC SUVmean_late, respectively. We obtained TBR_early by dividing the aortic SUVmax_early by SVC SUVmean_early and TBR_late by dividing aortic SUVmax_late by SVC SUVmean_late.

Statistical Analysis

Categorical data are presented as proportions/percentages. Continuous variables are presented as mean ± SD and/or median (range). We categorized patients into groups based on the time of the delayed imaging. We compared baseline clinical characteristics between patients' groups using Fisher's Exact χ^2 test and Analysis of variance (ANOVA). We used the Paired-Samples *t* test to compare early and late variables. We used the Pearson Correlation to check for correlation between the late parameters and the time the delayed imaging was acquired. We used Spearman Correlation to test for correlation between change in TBR, aortic SUVmax, and SVC SUVmean vs the time the delayed imaging was obtained. We then evaluated the changes in TBR, aortic SUVmax, and SVC SUVmean with delayed imaging time using Paired-Samples *t* test. We used simple and multiple linear regression to check if any of age, male gender, hypertension, smoking, or fasting blood sugar level could predict any of the quantitative parameters on the early and delayed imaging. We set statistical significance at a *P* value of < 0.05. We performed statistical analysis using SPSS statistics version 21.0 (IBM Corp., Armonk, NW, USA).

RESULTS

Among 64 eligible patients, 7 patients were excluded due to use of anti-inflammatory therapy ($n = 3$), presence of renal failure ($n = 2$), and refusal of patient to participate in the study ($n = 2$). A total of 57 patients were eventually included with a mean age of 45.93 ± 15.07 years. There were 33 females, and 23 were smokers. Twenty-one percent of patients were hypertensive, while 18 patients had well-controlled type II diabetes mellitus with a mean fasting blood sugar of 5.84 mmol/L for the whole group. All patients had normal-appearing arteries (aorta and other arteries) on CT with no foci of calcification. Table 1 shows the

Table 1. Baseline characteristics of the study participants

Variable	Frequency (N = 57)	Percent
Age (years)		
Mean ± SD	45.93 ± 15.07	
Sex		
Male	24	42.11
Female	33	57.89
Hypertension		
Yes	12	21.05
No	45	78.95
Diabetes mellitus		
Yes	10	17.54
No	47	82.46
Smoking		
Yes	23	40.35
No	34	59.65
Indications for ^{18}F-FDG PET/CT		
Evaluation for possible occult cancer	3	5.26
Re-staging post cancer therapy	27	47.37
Suspected cancer recurrence	15	26.32
Suspected fever of unknown origin	12	21.05
Fasting blood sugar (mmol/L)		
Mean ± SD	5.84 ± 0.73	
Range	4.40–7.00	
Time of delayed imaging		
Mean ± SD	142.74 ± 28.94	
Range	120.0–245.0	

detail baseline characteristics of the patients included in this study.

Impact of Delayed Imaging on Quantitative Parameters

The mean time between intravenous ^{18}F-FDG injection and the start of delayed imaging was 142.74 minutes (range 120.00-245.00). In 14 patients, delayed imaging was acquired at 120 minutes. Delayed imaging was acquired between 121 and 150 minutes in 29 patients, between 151 and 180 minutes in seven patients, and > 180 minutes in another seven patients. Baseline clinical characteristics were not significantly different among patients' groups by delayed imaging time (Table 2). Aortic SUVmax of the ascending aorta rose on the delayed imaging compared with the early imaging in all patients with a mean rise of 70%, $P < 0.001$ (Figure 1a). Conversely, there was a significant drop in SVC SUVmean in the delayed imaging compared with the early imaging with a mean decrease of 52%, $P < 0.001$ (Figure 1b). Delayed imaging showed a significant rise in TBR of 122% compared with the early imaging, $P < 0.001$ (Figure 1c). Table 3 shows the average aortic SUVmax, venous SUVmean, and TBR on the early and delayed imaging.

Correlation Between the Time of Delayed Imaging and the Change in Quantitative Parameters

Delayed imaging was acquired over a range of time in the participants, 120 to 245 minutes. We found a weak negative correlation between the SVC SUV-mean_late and the time of delayed imaging (Pearson correlation coefficient = − 0.298, $P = .025$). Similarly, we found a moderate positive correlation between TBR_late and the time of delayed imaging (Pearson correlation coefficient = 0.526, $P < .001$). Aortic SUVmax_late was not significantly correlated with the time of delayed imaging.

Consequently, SUVmean decreases while TBR increases with further delay in the time of delayed imaging beyond 120 minutes. The change in SUVmax with further delay in imaging time did not reach statistical significance. Table 4 shows the relationship between the time of delayed imaging and the TBR_late, SVC SUVmean_late, and aortic SUVmax_late. Figures 2a and b show the typical image of an early and delayed ^{18}F-FDG PET/CT imaging.

In a sub-group analysis evaluating the impact of the time of delayed imaging on changes TBR, aortic SUVmax, and SVC SUVmean, we found a progressive improvement in TBR obtained on the delayed imaging

Table 2. Comparison in the baseline characteristics of patients categorized according to the time of delayed imaging

	Time of imaging						
	120	121–150	151–180	> 180	Total		
Variable	*n* (%)	*n* (%)	*n* (%)	*n* (%)	*n* (%)	χ^2	*P* value
Age							
Mean ± SD	50.79 ± 13.53	45.48 ± 16.47	39.71 ± 13.63	44.29 ± 12.93		0.913[a]	.441
Gender							
Male	6 (42.9)	13 (44.8)	2 (28.6)	3 (42.9)	24 (42.1)	0.699	.952
Female	8 (57.1)	16 (55.2)	5 (71.4)	4 (57.1)	33 (57.9)		
Hypertension							
Yes	3 (21.4)	6 (20.7)	2 (28.6)	1 (14.3)	12 (21.1)	0.667	.961
No	11 (78.6)	23 (79.3)	5 (71.4)	6 (85.7)	45 (78.9)		
Smoking							
Yes	6 (42.9)	13 (44.8)	2 (28.6)	2 (28.6)	23 (40.4)	1.062	.871
No	8 (57.1)	16 (55.2)	5 (71.4)	5 (71.4)	34 (59.6)		
FBS							
Mean ± SD	5.86 ± 0.72	5.66 ± 0.71	6.20 ± 0.40	6.21 ± 0.95		1.844[a]	.150

χ^2, Fisher's Exact Chi square test; *FBS*, fasting blood sugar
[a]Analysis of variance (ANOVA)

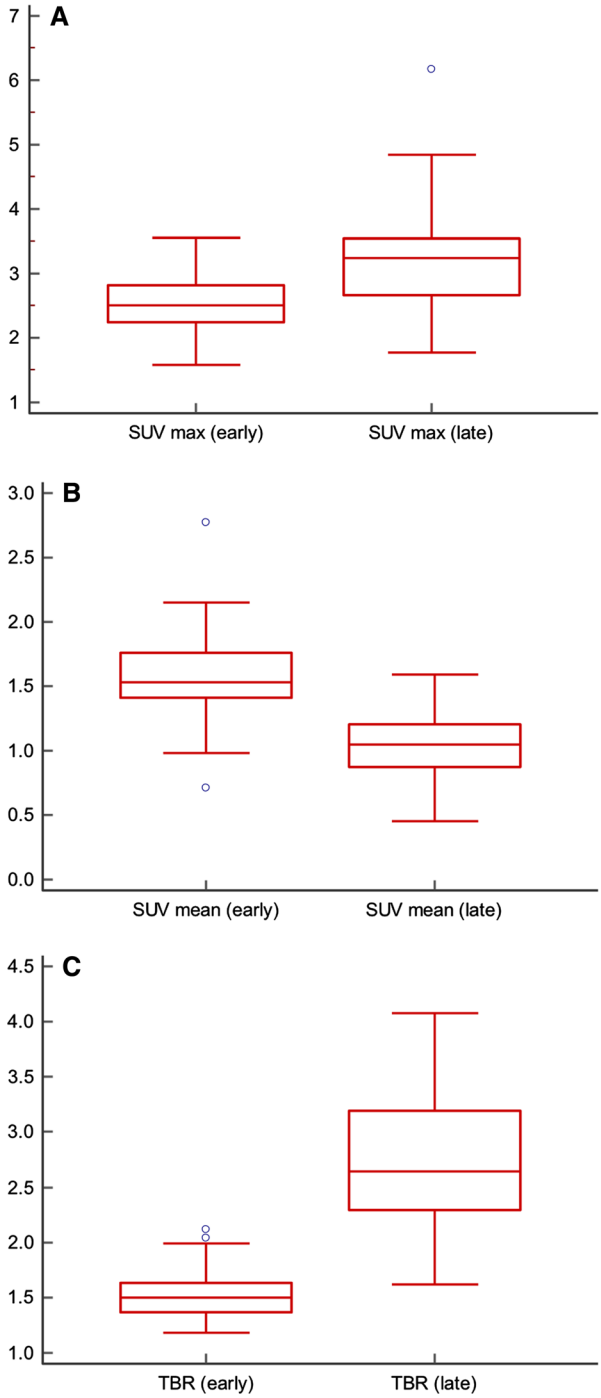

Figure 1. Box plots showing significant differences in (**A**) aortic SUVmax, (**B**) SVC SUVmean, and (**C**) aortic TBR between the early and delayed ^{18}F-FDG PET imaging. Aortic SUVmax increased by a mean of 70%; venous TBR decreased by a mean of 52% and TBR increased by a mean of 122% between early and delayed imaging, $P < .001$ in all cases.

at different time-points from 120 minutes to > 180 minutes ($P < .001$). SVC SUVmean also showed a progressive decline across all imaging time-points from 120 to beyond 180 minutes ($P < .005$). Aortic SUVmax significantly increased progressively from 120 minutes up till 180 minutes of imaging time-point. The improvement in aortic SUVmax beyond 180-minute imaging time-point did not reach a statistical significance. Table 5 shows the detailed changes in TBR, aortic SUVmax, and SVC SUVmean with the time of delayed imaging. Figure 3 is a graphical representation of the changes in then different quantitative parameters with increasing time of imaging.

Predictors of Quantitative Parameters

Among the factors (age, male gender, systemic hypertension, smoking history, and fasting blood sugar) tested for their abilities to predict the quantitative parameters on both the early and delayed imaging, history of hypertension was the most consistent in predicting aortic SUVmax and SVC SUVmean on the early and delayed imaging, $P < .05$. None of the factors tested was a significant predictor of TBR either on the early or delayed imaging. Table 6 shows the performance of the different factors tested in their abilities to predict the quantitative parameters on both the early and delayed imaging.

DISCUSSIONS

We applied optimum patients' preparation and PET imaging parameters to quantifying arterial ^{18}F-FDG uptake and found an improvement in the measured quantitative parameters. Arterial SUVmax, a marker of the intensity of ^{18}F-FDG uptake in the arterial wall, increased by a mean of 70%. This improvement in aortic SUVmax indicates an improvement in tracer uptake with improved imaging parameters and prolonged uptake time. SVC SUVmean, a marker of the blood-pool background activity, declined by 52% between the early un-optimized imaging and delayed imaging optimized for vascular inflammation imaging. TBR, a ratio of arterial SUVmax and venous SUVmean, showed a tremendous improvement of 122% between the un-optimized early imaging and the delayed imaging. Our data confirm that the application of the specific set of parameters recommended by the cardiovascular committee of the EANM is necessary for adequate quantification of ^{18}F-FDG uptake in the arterial wall.[13] Our results suggest that data from routinely acquired PET imaging for other indications may significantly underestimate the quantitation of vascular tracer uptake.

Many authors have identified difficulties with quantitation of vascular uptake of ^{18}F-FDG with a call to standardize patient preparation and imaging parameters.[8,9,14] Many studies have since been published

Table 3. Changes in aortic SUVmax, SVC SUVmean, and aortic TBR between early and delayed ^{18}F-FDG PET imaging

Variable	Duration (min) Timing	Mean ± SD	Range	Mean difference	95% Confidence interval Lower	Upper	t	*P* value
Aortic TBR	Early	1.53 ± 0.20	1.18–2.12	1.22	1.06	1.37	15.737	< .001*
	Late	2.75 ± 0.59	1.62–4.08					
SVC SUVmean	Early	1.57 ± 0.33	0.71–2.77	− 0.52	− 0.58	− 0.46	− 17.894	< .001*
	Late	1.04 ± 0.25	0.45–1.59					
Aortic SUVmax	Early	2.52 ± 0.43	1.58–3.56	0.70	0.54	0.86	8.802	< .001*
	Late	3.22 ± 0.75	1.77–6.17					

T, Paired-Samples *t* test
**P* value < .01

Table 4. Correlation between quantified parameters and the time of delayed imaging

Variables	Time of delayed imaging r_p	*P* value
TBR_late	.526	< .001*
SVC SUVmean_late	− .298	.025*
Aortic SUVmax_late	.136	.314
Change in parameters	r_s	
TBR	0.307	.003*
SVC SUVmean	− 0.271	.043*
Aortic SUVmax	− 0.144	.284

r_p, Pearson correlation coefficient; r_s, Spearman correlation coefficient
**P* value < .05

evaluating the feasibility and the optimum imaging conditions of vascular atheromatous inflammation in different arterial beds.[6,10,11,15] In a large study by Bucerius et al, there was an increase in the aortic TBR with increasing uptake time.[10] Unlike in our study, aortic SUVmax decreased with increased uptake time. A significant difference between this study and ours is that patients in our study were imaged at two-time-points using two different PET imaging parameters. The longer acquisition time of 8 minutes per bed position compared with the early imaging (acquired at 3 minutes per bed position) as well as reconstruction protocols on the delayed imaging optimized for vascular inflammation imaging (higher iterations, no post-filtering) contributed to reducing the impact of partial volume effect on the aortic SUVmax.[13] The CT parameters were similar for the early and delayed imaging. The increase in aortic SUVmax, decline in SVC SUVmean, and consequently increase in TBR, therefore, result from multiple factors including prolonged uptake time and optimized PET imaging parameters. Other factors such as activity of ^{18}F-FDG and blood sugar levels at the time of tracer injection which are known to influence the SUV parameters were similar for both imaging time-points.

Patients included in our study had their delayed imaging acquired at a variable time from 120 to 245 minutes. We determined the impact of further delay in acquiring PET imaging and found a significant decline in SVC SUVmean and an improvement in TBR across different delayed imaging time-points up till beyond 180 minutes. The increase in aortic SUVmax with delayed imaging was significant up till the 180-minute imaging time-point but not beyond. Our findings suggest that the increase seen in TBR when imaging is delayed beyond 180 minutes is due to an improvement in blood-pool background activity clearance without any significant improvement in arterial uptake of ^{18}F-FDG. The recommendation of the EANM cardiovascular imaging committee regarding the time of imaging is a compromise agreed on to achieved an acceptable image quality without making patients observe a long uptake time with a potential to disrupt the schedule of other patients being

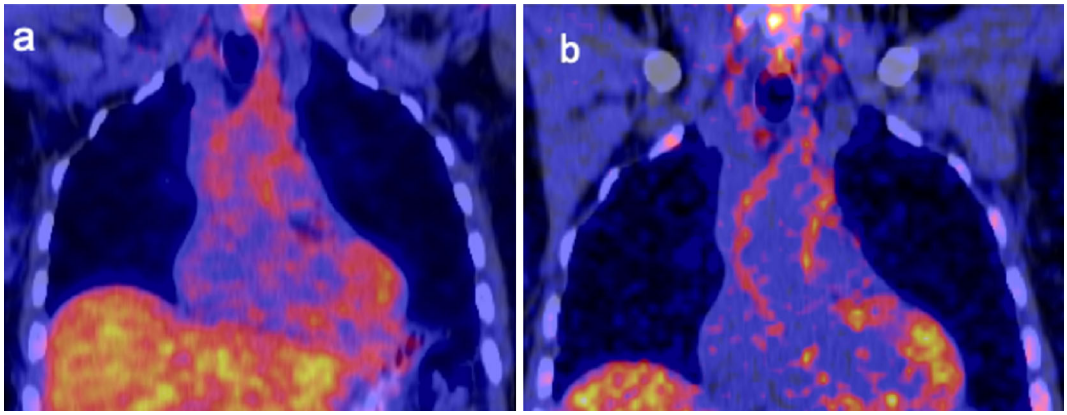

Figure 2. Coronal fused ^{18}F-FDG PET/CT imaged of a typical patient. The early image (**A**) shows tracer localization to the ascending aorta wall but with high blood-pool background activity. Delayed image (**B**) shows an increase in the intensity of tracer localized to the aortic wall with a much-improved clearance of background blood-pool activity.

Table 5. Changes in TBR, aortic SUVmax, and SVC SUVmean with the time of delayed imaging

Time of delay (min)	*n*	Early Mean ± SD	Late Mean ± SD	t	*P* value
TBR					
120	14	1.54 ± 0.18	2.68 ± 0.58	− 8.585	< .001*
121–150	29	1.53 ± 0.21	2.53 ± 0.43	− 11.110	< .001*
151–180	7	1.36 ± 0.07	3.06 ± 0.66	− 6.795	< .001*
> 180	7	1.68 ± 0.22	3.47 ± 0.43	− 11.132	< .001*
SVC SUVmean					
120	14	1.60 ± 0.18	1.10 ± 0.18	10.542	< .001*
121–150	29	1.57 ± 0.31	1.09 ± 0.24	13.745	< .001*
151–180	7	1.59 ± 0.55	0.94 ± 0.32	6.147	.001*
> 180	7	1.45 ± 0.40	0.85 ± 0.28	5.004	.002*
Aortic SUVmax					
120	14	2.55 ± 0.27	3.34 ± 0.54	− 6.467	< .001*
121–150	29	2.55 ± 0.46	3.15 ± 0.55	− 6.288	< .001*
151–180	7	2.34 ± 0.58	3.01 ± 1.02	− 3.381	.015*
> 180	7	2.54 ± 0.46	3.50 ± 1.39	− 2.271	.064

T, Paired-Samples T test
**P* value <0.05

imaged with the same PET/CT scanner for other indications. While our results support the compromised recommendation of the EANM that imaging for vascular inflammation is done after a 2-hour uptake time which is a better imaging time than an earlier imaging, a longer uptake time up till 180 minutes will be more ideal. In an early work by Tawakol et al, good TBR of atheromatous lesions was obtained on PET imaging done after a 3-hour uptake time.[15] In a study with a contrary finding, Menezes et al could not demonstrate a significant difference in arterial FDG uptake between imaging done at one and three hours post tracer injection. This study done in a limited number of patients with aortic aneurysm has some methodological differences with most studies published on this topic especially regarding the authors' choice of vessel for background correction.[16] Menezes and colleagues obtained their blood-

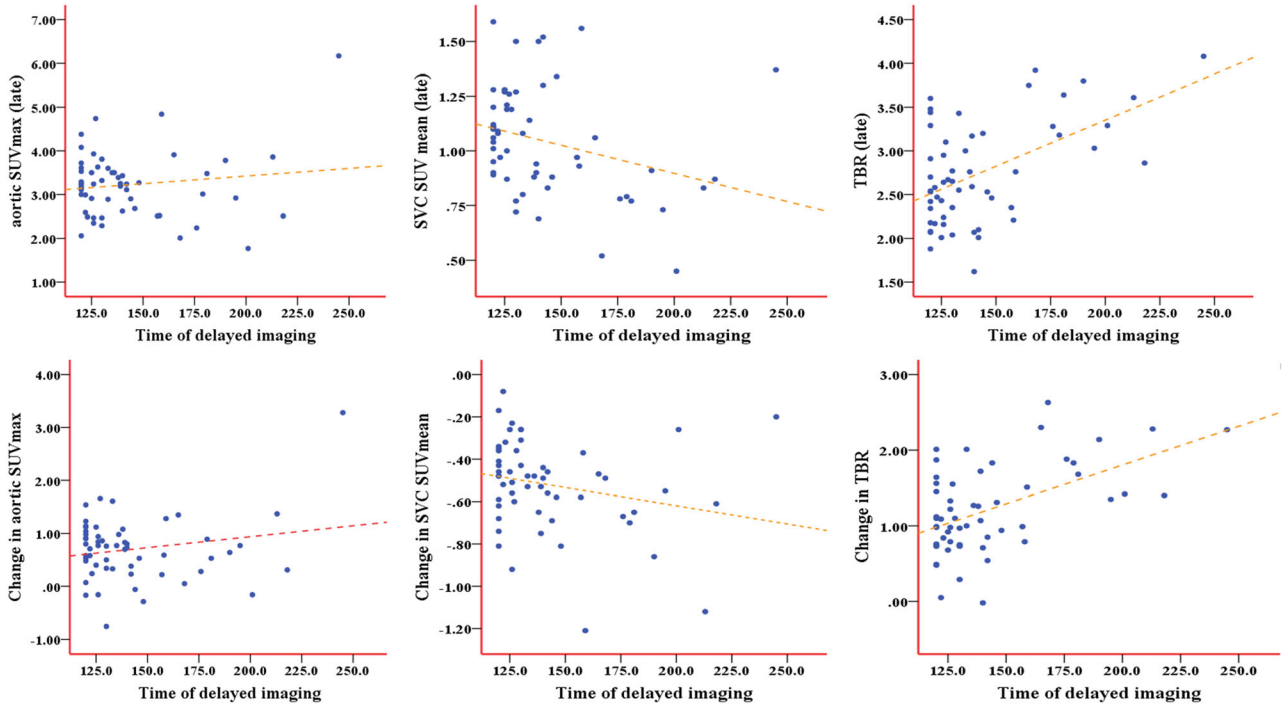

Figure 3. Scatter plots showing the changes of the time of delayed imaging on (top row from right to left) the TBR_late, SVC SUVmean_late, and aortic SUVmax_late. Scatter plots on the bottom row show the changes in (from right to left) the TBR, SVC SUVmean, and aortic SUVmax with the increasing time at which the delayed images were acquired.

pool background activity from the lumen of the diseased artery rather than from an adjacent vein.[16]

Among the factors we tested for their ability to predict the level of arterial ^{18}F-FDG uptake and blood-pool background activity clearance, systemic hypertension was the most consistent predictor in both simple and multiple linear regressions. Individuals with systemic hypertension generally have hypertrophied smooth muscle in their vessel wall. As an adaptive response to sustained elevated blood pressure, the vessels of hypertensive patients develop concentric thickening with luminal narrowing.[17] Increase in the thickness of arterial wall improves quantification of tracer uptake with it. Thinner vessels in younger individuals without cardiovascular disease are associated with a significant underestimation of arterial ^{18}F-FDG quantification.[9] We performed image analysis using the ascending aorta as the arterial bed of interest. The ascending aorta is a large artery with thick wall reducing the extent of the underestimation of the measured parameters that may be caused by partial volume effect. Others have shown that TBR measured are similar across different arterial territories.[18] Age was a significant predictor of early and late SVC SUVmean in a simple linear regression. This may be due to better renal function in younger individuals with prompt background activity clearance compared with older population. The impact of age lost its significance of multiple linear regression. Serum blood sugar at the time of ^{18}F-FDG administration had no impact on any of the parameters tested. This may be due to the strict fasting blood sugar level we used as an entry criteria for this study implying that patients we included were most likely non-diabetic or well-controlled diabetic patients. Male gender significantly predicts background clearance on the early image but not on the delayed image. We speculate that this finding may mean that males have an early rapid background activity clearance which equates with the clearance rate in females beyond 60 minutes.

Inflammation plays an important role in the formation and progression of vascular atheroma.[3] Agents with anti-inflammatory effects are now being evaluated for their potential for primary and secondary prevention of atherosclerotic cardiovascular diseases.[19] ^{18}F-FDG PET/CT holds a great potential for non-invasive evaluation of the effectiveness of these therapy agents.[20] They are, however, several drawbacks to the widespread clinical application of ^{18}F-FDG PET/CT for arterial

Table 6. Predictors of arterial SUVmax, SUV SUVmean, and TBR on early and delayed imaging

	Simple linear regression		Multiple linear regression	
Variables	**b (95% CI)**	***P* value**	**Adjusted b (95% CI)**	***P* value**
TBR early				
Age	− 0.004 (− 0.007 to 0.000)	**.038***		
Gender (male)	0.024 (− 0.087 to 0.134)	.670		
Hypertension	− 0.058 (− 0.191 to 0.075)	.385		
Smoking	0.019 (− 0.092 to 0.131)	.728		
FBS	− 0.046 (− 0.120 to 0.029)	.223		
TBR late				
Age	− 0.006 (− 0.016 to 0.005)	.287		
Gender (male)	− 0.073 (− 0.393 to 0.246)	.647		
Hypertension	− 0.003 (− 0.402 to 0.395)	.987		
Smoking	− 0.248 (− 0.562 to 0.067)	.121		
FBS	0.062 (− 0.156 to 0.280)	.573		
SVC SUVmean (early)				
Age	0.008 (0.002 to 0.013)	**.007***	0.004 (− 0.002 to 0.009)	.117
Gender (male)	− 0.223 (− 0.390 to − 0.056)	**.010***	− 0.173 (− 0.335 to − 0.011)	**.037***
Hypertension	0.377 (0.187 to 0.566)	**< .001***	0.299 (0.100 to 0.498)	**.004***
Smoking	− 0.175 (− 0.347 to − 0.002)	**.047***	− 0.027 (− 0.194 to 0.140)	.747
FBS	0.070 (− 0.049 to 0.189)	.243		
SVC SUVmean (late)				
Age	0.005 (0.001 to 0.010)	**.027***	0.003 (− 0.002 to 0.007)	.229
Gender (male)	− 0.129 (− 0.262 to 0.004)	.057		
Hypertension	0.300 (0.150 to 0.451)	**< .001***	0.268 (0.109 to 0.427)	**.001***
Smoking	− 0.080 (− 0.217 to 0.057)	.246		
FBS	0.017 (− 0.077 to 0.111)	.717		
Aortic SUVmax (early)				
Age	0.007 (− 0.001 to 0.014)	.085		
Gender (male)	− 0.266 (− 0.489 to − 0.042)	**.021***	− 0.163 (− 0.385 to 0.059)	.148
Hypertension	0.404 (0.141 to 0.666)	**.003***	0.324 (0.068 to 0.580)	**.014***
Smoking	− 0.335 (0.553 to − 0.011)	**.003***	− 0.205 (− 0.435 to 0.024)	.079
FBS	− 0.014 (− 0.174 to 0.145)	.856		
Aortic SUVmax (late)				
Age	0.003 (− 0.011 to 0.016)	.703		
Gender (male)	− 0.405 (− 0.795 to − 0.014)	**.042***	− 0.251 (− 0.648 to 0.147)	.211
Hypertension	0.639 (0.179 to 1.098)	**.007***	0.521 (0.062 to 0.980)	**.027***
Smoking	− 0.504 (− 0.889 to − 0.120)	**.011***	− 0.299 (− 0.711 to 0.112)	.150
FBS	0.076 (− 0.199 to 0.350)	.582		

b Coefficient of Linear regression)
SVC SUVmean (early): R^2: 0.338; SVC SUVmean (late): R^2: 0.249; aortic SUVmax (early): R^2: 0.266; aortic SUVmax (late): R^2: 0.212
*P value $< .05$

inflammation imaging. The most significant of these drawbacks is the lack of specificity of ^{18}F-FDG. Within the atheromatous lesion, ^{18}F-FDG is taken up by the inflammatory cells and the hypertrophied vascular smooth muscle cells as well. Similarly, there is high physiologic ^{18}F-FDG uptake in the myocardium and soft tissues of the neck which may compromise quantification of arterial ^{18}F-FDG uptake in the coronary and carotid arteries, respectively. There are now concerted efforts to develop more specific tracers which do not suffer from these drawbacks experienced with ^{18}F-FDG use.[3,21,22]

Our study is unique in the fact that we compared two sets of imaging conditions, one optimized for vascular inflammation imaging and the other not, in the same set of patients in a test-retest setting. Our study design allows for each patient to serve as their own control which removes inter-individual variability as a confounding factor. Despite this, our study suffers from some limitations including the group of patients we studied. Our patients have apparently healthy aortas without atheromatous lesions. Also, we did not fully characterize the cardiovascular risk of our patients, and hence we could not perform a sub-group analysis of our study population based on their cardiovascular risk grouping. These limitations of our study must be borne in mind while applying our findings to imaging of atheromatous lesions in patients with established cardiovascular diseases. We recruited a modest study population due to the radiation burden patients were exposed to in this test-retest study design. Despite this modest study population, we performed sub-group analyses on the patients categorized according to the time of delayed imaging and found statistically significant differences in the quantified parameters between groups in most cases. Only one reader performed image analysis in this study. This was based on the widely acknowledged excellent inter-observer agreement in vascular ^{18}F-FDG uptake quantification informing a single-reader image analysis in some recent studies.[7,10,18] Image analysis by two readers has also been reported in recent studies and its application could have provided a more robust quantification of vascular ^{18}F-FDG uptake in this study.[23]

CONCLUSION

Vascular inflammation imaging with ^{18}F-FDG PET requires optimized imaging conditions. These imaging conditions enable improved vascular quantification through increased vascular tracer uptake and improved blood-pool background activity clear.

NEW KNOWLEDGE GAINED

Application of the ^{18}F-FDG PET imaging conditions recommended by the cardiovascular committee of the EANM leads to an improvement in quantified arterial tracer uptake and better background clearance. There is an increase in arterial ^{18}FDG uptake and venous blood-pool clearance up till 180 minutes post tracer injection. Delaying imaging beyond 180 minutes post tracer injection leads to further improvement of blood-pool background activity clearance but not an increase in vascular ^{18}F-FDG uptake.

Acknowledgments

IOL is a PhD student at the time this study was performed. He receives a monthly stipend from the Nuclear Medicine Research Infrastructure (NuMeRI) hosted at the Department of Nuclear Medicine, University of Pretoria. All authors wish to thank members of staff at the Department of Nuclear Medicine, Stve Biko Academic Hospital and University of Pretoria, Pretoria, South Africa.

Disclosures

Ismaheel O. Lawal, Kgomotso G. Mokoala, Gbenga O. Popoola, Thabo Lengana, Alfred O. Ankrah, Anton C. Stoltz, and Mike M. Sathekge declare that they have no conflict of interest.

References

1. Roth GA, Abate D, Abate KH, Abay SM, Abbafati C, Abbasi N, et al Global, regional, and national age-sex-specific mortality for 282 causes of death in 195 countries and territories, 1980-2017: A systematic analysis for the Global Burden of Disease Study 2017. Lancet 2018;392:1736-88.
2. Libby P. Inflammation and cardiovascular disease mechanisms. Am J Clin Nutr 2016;83:456S-60S.
3. Lawal IO, Ankrah AO, Stoltz AC, Sathekge MM. Radionuclide imaging of inflammation in atherosclerotic vascular disease among people living with HIV infection: Current practice and future perspective. Eur J Hybrid Imaging 2019;3:5.
4. Lawal I, Sathekge M. F-18 FDG PET/CT imaging of cardiac and vascular inflammation and infection. Br Med Bull 2016;120:55-74.
5. Lawal IO, Ankrah AO, Popoola GO, Lengana T, Sathekge MM. Arterial inflammation in young patients with human immunodeficiency virus infection: A cross-sectional study using F-18 FDG PET/CT. J Nucl Cardiol 2018. https://doi.org/10.1007/s12350-018-1207-x.
6. Rudd JHF, Warburton EA, Fryer TD, Jones HA, Clark JC, Antoun N, et al Imaging atherosclerotic plaque inflammation with [^{18}F]-Fluorodeoxyglucose positron emission tomography. Circulation 2002;105:2708-11.
7. Figueroa AL, Abdelbaky A, Truong QA, Corsini E, MacNabb MH, Lavender ZR, et al Measurement of arterial activity on routine FDG PET/CT images improves prediction of risk of future CV event. JACC Cardiovasc Imaging 2013;6:1250-9.
8. Huet P, Burg S, Le Guludec D, Hyafil F, Buvat I. Variability and uncertainty of 18F-FDG PET imaging protocols for assessing inflammation in atherosclerosis: Suggestions for improvement. J Nucl Med 2015;56:552-9.
9. Burg S, Dupas A, Stute S, Dieudonné A, Huet P, Le Guludec D, et al Partial volume effect estimation and correction in the aortic vascular wall in PET imaging. Phys Med Biol 2013;58:7527-42.
10. Bucerius J, Mani V, Moncrieff C, Machac J, Fuster V, Farkouh ME, et al Optimizing 18F-FDG circulation time, injected dose, uptake parameters, and fasting blood sugar levels. Eur J Nucl Med Mol Imaging 2014;41:369-83.
11. Blomberg BA, Thomassen A, Takx RA, Hildebrandt MG, Simonsen JA, Buch-Olsen KM, et al Delayed 18F-fluorodeoxyglucose PET/CT imaging improves quantification of

atherosclerotic plaque inflammation: Results from the CAMONA study. J Nucl Cardiol 2014;21:588-97.
12. Subramanian S, Tawakol A, Burdo TH, Abbara S, Wei J, Vijayakumar J, et al Arterial inflammation in patients with HIV. JAMA 2012;308:379-86.
13. Bucerius J, Hyafil F, Verberne HJ, Slart RHJA, Linder O, Sciagra R, et al Position paper of the Cardiovascular Committee of the European Association of Nuclear Medicine (EANM) on PET imaging of atherosclerosis. Eur J Nucl Med Mol Imaging 2016;43:780-92.
14. Sadeghi MM. ^{18}F-FDG PET and vascular inflammation; time to reflect the paradigm? J Nucl Cardiol 2015;22:319-24.
15. Tawakol A, Migrino RQ, Bashian GG, Bedri S, Vermylen D, Cury RC, et al In vivo 18F-fluorodeoxyglucose positron emission tomography imaging provides a noninvasive measure of carotid plaque inflammation in patients. J Am Coll Cardiol 2006;48:1818-24.
16. Menezes LJ, Kotze CW, Hutton BF, Endozo R, Dickson JC, Cullum I, et al Vascular inflammation imaging with 18F-FDG PET/CT: When to image? J Nucl Med 2009;50:854-7.
17. Mitchell RN. Blood vessels. In: Kumar V, Abbas AK, Aster JC, editors. Robins and Cotran pathologic basis of disease. 9th ed. Saunders Elsevier: Philadelphia; 2015. p. 483-522.
18. Knudsen A, Hag AMF, Loft A, von Benzon E, Keller SH, Møller HJ, et al HIV infection and arterial inflammation assessed by ^{18}Ffluorodeoxyglucose (FDG) positron emission tomography (PET): A prospective cross-sectional study. J Nucl Cardiol 2015;22:372-80.
19. Ridker PM, Everett BM, Thuren T, MacFadyen JG, Chang WH, Ballantyne C, et al Antiinflammatory therapy with canakinumab for atherosclerotic disease. N Engl J Med 2017;377:1119-31.
20. Hsue PY, Li D, Ma Y, Ishai A, Manion M, Nahrendorf M, et al IL-1ß inhibition reduces atherosclerotic inflammation in HIV infection. JACC 2018;72:2809-10.
21. Vigne J, Thackeray J, Essers J, Makowski M, Varasteh Z, Curaj A, et al Current and emerging preclinical approaches for imaging-based characterization of atherosclerosis. Mol Imaging Biol 2018;20:869-87.
22. Bucerius J, Dijkgraaf I, Mottaghy FM, Schurgers LJ. Target identification for the diagnosis and intervention of vulnerable atherosclerotic plaques beyond ^{18}F-fluorodeoxyglucose positron emission tomography imaging: Promising tracers on the horizon. Eur J Nucl Med Mol Imaging 2019;46:251-65.
23. Toczek J, Hillmer AT, Han J, Liu C, Peters D, Emami H, et al FDG PET imaging of vascular inflammation in post-traumatic stress disorder: A pilot case-control study. J Nucl Cardiol 2019. https://doi.org/10.1007/s12350-019-01724-w.